International Journal of Engineering Trends and Technology
ISSN: 2231 – 5381 / https://doi.org/10.14445/22315381/IJETT-V70I8P217

Volume 70 Issue 8, 166-171, August 2022

Original Article

Accuracy of Cell-Centre Derivation of Unstructured-Mesh Finite Volume Solver

Adek Tasri

Mechanical Engineering Department, Universitas Andalas, Indonesia

adek.tasri@eng.unand.ac.id

Received: 11 June 2022 Revised: 29 July 2022 Accepted: 09 August 2022 Published: 22 August 2022

Abstract *- This study compared the accuracy of existing and a proposed second-order least square based cell centre derivation of velocity within an unstructured mesh finite volume solver. We tested the algorithms in isolation on ideal data to determine their basic numerical accuracy on good quality and artificially distorted meshes. The study found that the least-square-based cell centre derivations were more accurate than Gauss divergence-based derivations. The preliminary interpolation stage in cell centre derivation increased L1 error and reduced the order of accuracy in the distorted mesh. The second-order least square-based cell centre derivations were the most accurate among the methods tested in this study. The Frink's cell centre derivation was the least accurate.*

Keywords *- Finite volume, Cell centre derivation, Unstructured mesh.*

1. Introduction

Unstructured and cell-centred finite volume solvers have great popularity in solving the general transport equation of heat and mass flow because of the ability of the methods to model actual engineering flow in complex domains [1] [2] [3]. However, the finite volume method still needs improvement, especially in terms of convergence and accuracy. Many things influence the accuracy of the finite volume method, one of them flows variable derivation at cell centres. The cell centre derivation in the unstructured mesh is generally based on the Gauss divergence theorem introduced by Bart and Jespersen [4]. The other is based on the least-squares approximation of local Taylor series expansions described by Anderson and Bonhaus [5]. Anderson's least square-based methods were then improved by White [6] using a weighing function. Nishikawa [7] used two gradient-stencil augmentation techniques in the least square-based derivation to overcome the stability issue of the finite volume solver. Athkuri [8] improved the Gauss divergence-based derivation by using an axillary cell around the cell interest; the gradient at the cell centre was then calculated using the face centre data of the auxiliary cell—the method known as the Circle Green Gauss (CGG) methods. The procedures were later improved by Athkuri [9] by reducing the complexity of the implementation of CGG.

Aftosmis et al. [10] compared the Gauss divergence and the least square-based methods. They found the least square-based approach was better than the Green-Gauss-based method in the distorted mesh. Mavriplis [11] found Gauss divergence base derivation more accurate than least square based derivation in the highly stretched mesh. Correa et al. [12] and Syrakos [13] found Gauss divergence-based derivations have poor performance for poorly shaped elements. Diskin [14] compared the effect of several cell centre derivations on inviscid flow solution and suggested that cell-centred nearest-neighbour derivation with smart augmentation of the LSQ stencil was the best choice for curved geometry.

Some researchers have compared several cell centre derivation methods using certain test cases, and others have compared other methods with different test cases. The difference in test cases causes difficulties in determining the best among the existing methods. In this study, several cell derivation methods were compared using a flow past circular cylinder as a test case. This test case was chosen because of the availability of analytical solutions, and the flow has strong velocity gradients representing most of the fluid flow conditions. A second-order least square-based cell centre derivation was also proposed in this study.

2. Methods for the derivation of flow variables at cell centres

In the Navier-Stokes solver, two distinct algorithms have evolved for cell derivation evaluation on unstructured meshes: one, introduced by Barth and Jespersen [4], based on Gauss's divergence theorem, and the other based on least-squares approximation of local Taylor series expansions, as described by Anderson and Bonhaus [5]. Both methods are presented briefly in this section.

2.1. Determination of cell-centre derivation using Gauss's divergence theorem

Gauss's divergence theorem applies to a closed region V of space R bounded by a smooth surface A. If $\vec{q}$ is a smooth vector field over R, and $\vec{n}$ is an outward-facing unit vector locally normal to element dA of the surface, then

$$\int_R \nabla \cdot \vec{q}\, dV = \int_S \vec{q} \cdot \vec{n}\, dS \quad (1)$$

Gauss's theorem may also be applied to a scalarφin the form

$$\int_R \nabla \varphi\, dV = \oint_S \varphi\, \vec{n}\, dA \quad (2)$$

and so the average value of the gradient $\nabla\varphi$ over the elementary volume dV is given by

$$\overline{\nabla\varphi} = \frac{1}{dV}\oint_S \varphi\, \vec{n}\, dA \quad (3)$$

For the volume that has a finite number of plane faces, the surface integral φin Equation (3) can be estimated using second order accurate midpoint rule

$$\nabla\varphi \approx \frac{1}{\Delta V}\sum_{i=1}^{i=k} \varphi_{f_i}\, \vec{n}_i\, \Delta A_i \quad (4)$$

where, $\vec{n}_i$ and $\Delta A_i$are normal vectors and area of the surface. $\varphi_{f_i}$is the interpolated value φ at the centre of $i^{th}$the face. Although the overbar has been dropped for simplicity, the gradient in Equation (4) is still a mean value for the element considered, so the representation is first-order accurate.

Barth and Jespersen were the first workers to apply this numerical technique to gradient determination on unstructured meshes [4]. Working in two dimensions, they defined two regions around a mesh cell to apply Equation (4), as shown in Figure 1. The first region was triangular, with its vertices corresponding to cell centres for the grid cell's immediate or "face neighbour" cells for which the gradient was to be determined c_0. The second region suggested was polygonal, linking cell centres at all cells which shared a vertex with the gradient cell c_0. By arranging the boundaries of these regions to link cell centres, where φ values are known as the face centre value, φ_{f_i}in

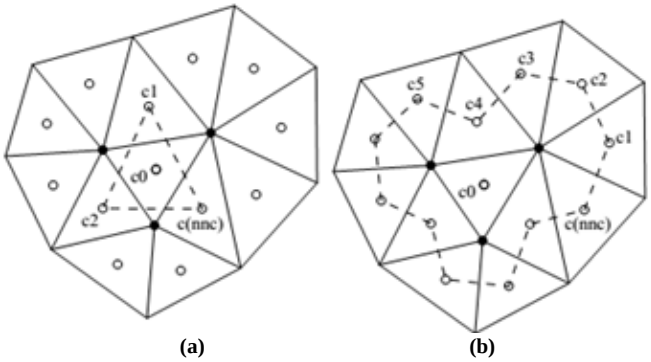

(a) **(b)**

Fig. 1 Barth and Jespersen integration regions for Gauss's theorem

Equation(4) can be estimated as the average of φ cells connected by face i^{th}. Barth and Jespersen rejected the simple triangular integration region, as in Figure 1a, because it could degenerate for highly skewed meshes and adopted the more complex stencil as in Figure 1b.

To simplify the boundary definition, both Frink [15] and Mathur and Murthy [16] used an integration region that corresponded exactly to the grid cell for which the gradient was determined. To perform the face summations on the right-hand side of Equation (4) $\varphi_{f_i}$was estimated as the average of φ the vertices connected by the face i^{th}. Mathur and Murthy determined φ the vertex from φ at the cell center around the vertex using inverse distance interpolation, while Frink used simple average interpolation.

2.2. Determination of cell-centre gradient by least-squares

An alternative method for computation of cell centre gradient value, based solely on cell centre values φ, uses a least-square approach. In the method, only φ values for the local cell centre $c_0$and its immediate edge neighbours are used to provide a compact stencil, though additional points could be included.

Referring to Figure 2, the first order expansion for$\tilde{\varphi}_{ci}$, the approximate value at cell centre ci is

$$\tilde{\varphi}_{c_i} \approx \varphi_{c_0} + \left(\frac{\partial\varphi}{\partial x}\right)_{c_0} \Delta x_i + \left(\frac{\partial\varphi}{\partial y}\right)_{c_0} \Delta y_i \quad i = 1\ldots k \quad (5)$$

The subscript indicates values at the central point, whilst and are the components of the vector displacement between the cell centre and the cell centre c_i. k is the number of the cell immediately around the cell c_0. The true value at the cell centre c_i is known, so the local error is

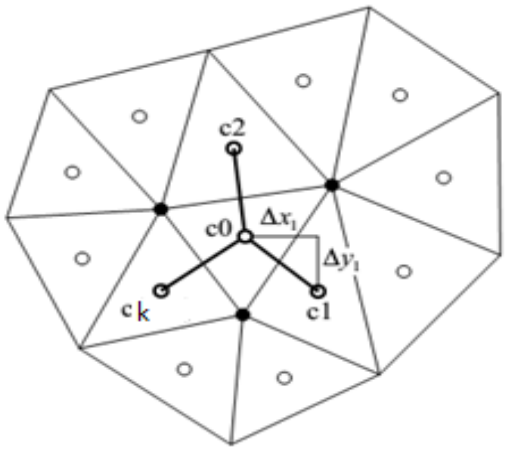

Fig. 2 Compact stencil for gradient determination by least-squares

$$\varepsilon_{c_i} = \varphi_{c_i} - \varphi_{c_0} - \left(\frac{\partial\varphi}{\partial x}\right)_{c_0} \Delta x_i - \left(\frac{\partial\varphi}{\partial y}\right)_{c_0} \Delta y_i \quad i = 1..k \quad (6)$$

Eq.(6) provides k equations, in this case, 3, with 2 unknowns derived φ at the cell centre. Thus a least-squares solution is required to minimise the sum of the squares of the error terms. The normal equations for this least-squares approximation may be written in matrix form as

$$A^T A\, x = A^T\, b \tag{7}$$

where

$$A = \begin{bmatrix} \Delta x_1 & \Delta y_1 & 1 \\ \Delta x_2 & \Delta y_2 & 1 \\ \vdots & \vdots & \vdots \\ \Delta x_{n_c} & \Delta y_{n_c} & 1 \end{bmatrix} \tag{8}$$

$$x = \begin{bmatrix} \left(\frac{\partial \varphi}{\partial x}\right)_{c_0} \\ \left(\frac{\partial \varphi}{\partial x}\right)_{c_0} \end{bmatrix} \tag{9}$$

and

$$b = \begin{bmatrix} \varphi_{c_1} - \varphi_{c_0} \\ \varphi_{c_2} - \varphi_{c_0} \\ \vdots \\ \varphi_{c_{nc}} - \varphi_{c_0} \end{bmatrix} \tag{10}$$

However, the normal equations are prone to ill-conditioning, so a direct solution of Equation (7) is not recommended. Instead, the matrix *A* is decomposed into an orthogonal matrix *Q* and an upper triangular matrix *R*. Gram-Schmidt decomposition method [17] was used in this work. Using this *QR* decomposition, the normal equations may be solved as [18]:

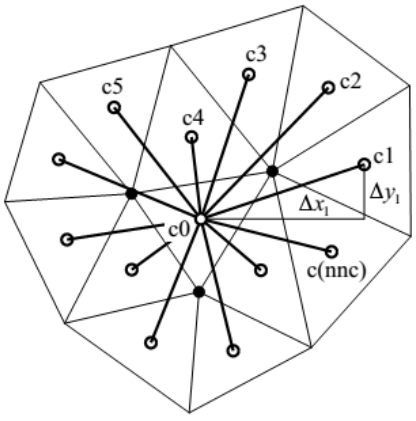

Fig. 3 Extended stencil for higher order derivative determination by least-squares

$$x = R^{-1} Q^T b \tag{11}$$

The least-squares method may be extended to second-order accuracy by including second- order terms in the truncated Taylor series used to estimate the approximate scalar value $\tilde{\varphi}_{c_i}$ at neighbour cell centres, such asc_i in Figure 9.

$$\tilde{\varphi}_{c_i} \approx \varphi_{c_0} + \left(\frac{\partial \varphi}{\partial x}\right)_{c_0} \Delta x_i + \left(\frac{\partial \varphi}{\partial y}\right)_{c_0} \Delta y_i + \frac{1}{2!}\left(\frac{\partial^2 \varphi}{\partial x^2}\right)_{c_0} {\Delta x_i}^2 + \left(\frac{\partial^2 \varphi}{\partial x \partial y}\right)_{c_o} \Delta x_i \Delta y_i + \frac{1}{2!}\left(\frac{\partial^2 \varphi}{\partial y^2}\right)_{c_0} {\Delta y_i}^2 \tag{12}$$

As previously mentioned, the error ε_{c_i} between this approximation and the known value of φ at $c_i$may be found, and the sum of the squares of such errors taken over all neighbour cells c_i to c_k may be minimised to give a least-squares solution for the derivatives at the cell centrec_0. The number of neighbour cells used must exceed the number of unknowns, which is now 5, so immediate "face neighbours" are no longer sufficient. Instead, the neighbours are taken as all cells which share a vertex with the cell c_0, as shown in Figure 3. Solution of the least-squares equations is again obtained by the *QR* reduction method of Equation (12), but now

$$A = \begin{bmatrix} \Delta x_1 & \Delta y_1 & 0.5{\Delta x_1}^2 & \Delta x_1 \Delta y_1 & 0.5{\Delta y_1}^2 \\ \Delta x_2 & \Delta y_2 & 0.5{\Delta x_2}^2 & \Delta x_2 \Delta y_2 & 0.5{\Delta y_2}^2 \\ \vdots & \vdots & \vdots & \vdots & \vdots \\ \Delta x_{n_c} & \Delta y_{n_c} & 0.5{\Delta x_{n_c}}^2 & \Delta x_{n_c} \Delta y_{n_c} & 0.5{\Delta y_{n_c}}^2 \end{bmatrix} \tag{13}$$

and

$$x = \begin{bmatrix} \left(\frac{\partial \phi}{\partial x}\right)_{c_0} \\ \left(\frac{\partial \phi}{\partial y}\right)_{c_0} \\ \left(\frac{\partial^2 \phi}{\partial x \partial x}\right)_{c_0} \\ \left(\frac{\partial^2 \phi}{\partial x \partial y}\right)_{c_0} \\ \left(\frac{\partial^2 \phi}{\partial y \partial y}\right)_{c_0} \end{bmatrix} \tag{14}$$

3. Comparison of cell centre derivative

In this study, the cell centre gradient algorithms were tested in isolation rather than their effect when used in governing equation solver. The algorithm's accuracy was determined by comparing the cell centre derivative of fluid velocity from the tested algorithm with the test-case analytic

solution in the form of the *L1* norm of the errors. The past flow cylinder was used as a test case. The analytical solution of the flow was determined by modelling the flow as a superimposed source and sink of equal strength [19].

The test case domain has a mesh with three different amounts of three angular cells of 1364, 11976 and 131898. The mesh was created by Delaunay triangulation with an equal face length at the boundary domain. To simulate the performance cell centre derivation algorithm in distorred mesh, a randomised mesh was produced by a randomly perturbed vertex coordinate. The calculation domain with 1364 cell standard and randomised meshes is shown in Figure 4.

Figure 5 compares the performance of the cell centre derivative algorithms in the standard mesh. The figure shows that Frink, Bart and Jespersen (BJ), Mathur and Murthy (MM), and the first order least square (FLS) based cell centre derivation have approximately first-order accuracy for the good quality standard mesh, with little to choose between them in terms of absolute error.

However, more significant differences are evident for the randomised mesh, as shown in Figure 6. Frink and the MM cell centre derivation exhibit increased absolute error values and were significantly poorer than first-order error reduction with grid refinement. This condition was due to the cell centre derivation algorithms involving a preliminary inverse interpolation from the cell centre to the cell vertex only having first-order accuracy in standard mesh

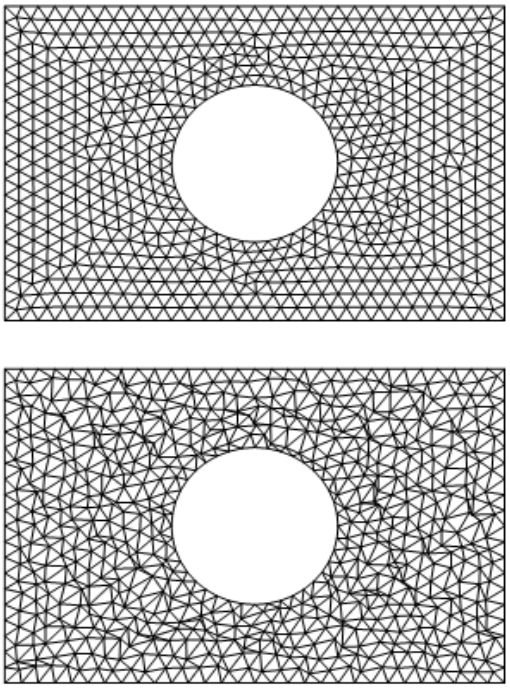

Fig. 4 Standard (top) and randomised (bottom) test meshes (Tasri, 2021a, 2021b)

as reported by Tasri [3] and Wang [20]. A similar condition was reported by Diskin [21], who found that the cell centre derivation that involves node averaging has only first-order accuracy. The errors of the inverse distance interpolation can be shown by writing φat a vertex as an interpolated of φ at cells around the vertex.

$$\varphi_v = \frac{\sum_{i=1}^{n} \frac{1}{l_i} \varphi_i}{\sum_{i=1}^{n} \frac{1}{l_i}} \tag{15}$$

Where l_i represents a Euclidean distance from cell *i* to vertex *v*. While φ_i can be determined using Taylor series expansion φat the vertex *v*

$$\varphi_i = \varphi_{ve} + \Delta x_i \frac{\partial \varphi_i}{\partial x} + \Delta y_i \frac{\partial \varphi_i}{\partial y} + O(\Delta^2) \tag{16}$$

Where φ_{ve} is the exact value of φ at the vertex *v*. $\varphi_v - \varphi_{ve}$ is the error of the inverse distance interpolation. The error can be determined by substituting φ_i in Equation (15) with Equation (16), yield:

$$\varphi_v - \varphi_{ve} = \frac{\partial \varphi}{\partial x} \frac{\sum_{i=1}^{n} (\Delta x_i \frac{1}{d_i})}{\sum_{i=1}^{n} (\frac{1}{d_i})} + \frac{\partial \varphi}{\partial y} \frac{\sum_{i=1}^{n} (\Delta y_i \frac{1}{d_i})}{\sum_{i=1}^{n} (\frac{1}{d_i})} + O(\Delta^2) \tag{17}$$

Equation (17) shows that $\varphi_v$is second-order accurate if the conditions in Equations (18) and (19) are satisfied:

$$\sum_{i=1}^{n} \Delta x_i \frac{1}{d_i} = 0 \tag{18}$$

$$\sum_{i=1}^{n} \Delta y_i \frac{1}{d_i} = 0 \tag{19}$$

The second-order accurate condition in Equations (18) and (19) will only be met if cell centres are evenly distributed around the vertices. This condition is only possible if a rectangular structured mesh is used. The cell centre is randomly distributed in an unstructured mesh so that the accuracy will be less than second-order. The interpolation error increases if the mesh is distorted. Thus, the error of the cell centre derivation algorithms involving a preliminary interpolation also increases. In contrast, FLS and BJ do not involve the preliminary interpolation and exhibit very little increasing error in the distorted mesh.

The first order least-squares method shows almost identical results with the best Gauss's theorem algorithm due to BJ, the differences being less than plotting accuracy.

The second order least-squares (SLS) based method returns a truly second order increase in accuracy with grid refinement, at least with this ideal data, and a significant decrease in absolute error level.

Based on these results, the least-squares methods appear to offer significant advantages. The first order least-squares scheme seems slightly more accurate than the best of Gauss's theorem methods, is at least as efficient in terms of storage requirements and arithmetic operation count, and is very easy for the programmer. In common with all the least-squares methods, the sensitivity to mesh distortion is very low, whilst modifications at mesh boundaries are relatively easily handled.

Using the QR algorithm to solve the least-squares equations, least-square-based cell centre derivations are efficient and robust. For the limited range of test cases studied, the present authors did not encounter any degeneration problems or ill-conditioning suggested in previous work, even when using randomised meshes. If cell distortion is large enough for such problems to appear, other aspects of the CFD solution are likely to be inadequate.

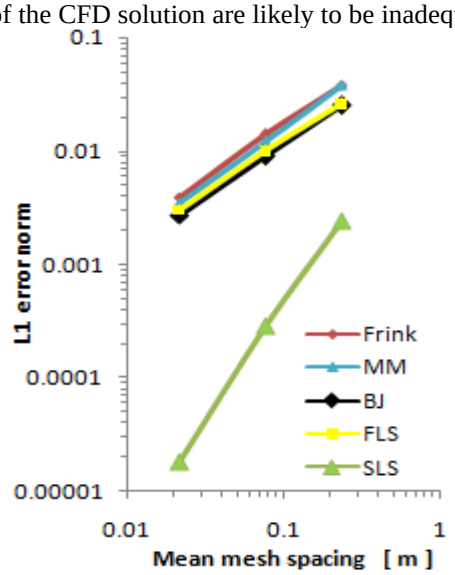

Fig. 5 The *L1* error of cell centre derivative of velocity in standard mesh

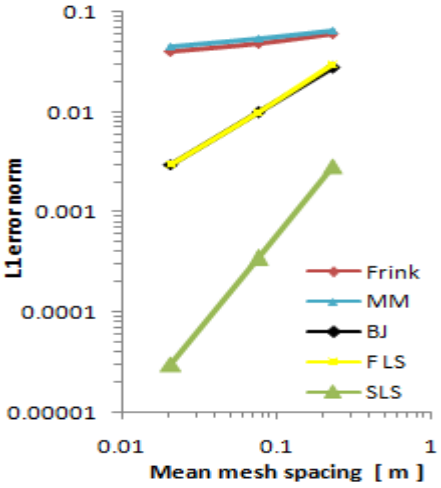

Fig. 6 The *L1* error of cell centre derivative of velocity in distorted mesh

4. Conclusion

The accuracy of cell centre derivation algorithms was tested in this study. Based on the test data, the following conclusions may be drawn:

1. The least-squares-based cell centre derivations and Barth and Jespersen's derivation operate directly on the stored data at cell centres without a preliminary interpolation stage. The algorithms were more accurate than those relying on a preliminary interpolation stage. *Mesh quality did not affect the L1 error and order of accuracy of the algorithms*.

2. The first order least-square based cell centre derivation and Bart and Jespersen's derivation have similar *L1* errors and order of accuracy for standard and distorted mesh.

3. The second-order least-square-based cell centre derivation has the lowest *L1* error and the highest order of accuracy among the algorithm tested in this study. The Frink's cell centre derivation was the least accurate.

4. Compared to Gauss divergence-based derivation, the least square base derivation has a lower error.

Author contribution statement

A. Tasri: Conceived and designed the numerical experiments; wrote the computer code used in the numerical experiment; Performed the experiments; Analysed and interpreted the data; analysed tools or data; Wrote the paper.

Data availability statement

Data included in article/supplementary material/referenced in the article.

Acknowledgements

The authors would like to express special thanks of gratitude to Dr. Ian Potts (University of Newcastle Upon Tyne, UK) for his advice on research.

References

[1] J. A. White, H. Nishikawa and R. Baurle, "Weighted Least-squares Cell-Average Gradient Construction Methods for the VULCAN-CFD Second-Order Accurate Unstructured Grid Cell-Centered Finite-Volume Solver," in AIAA Scitech Forum, San Diego, 2019.

[2] A. Tasri, A. Susilawati, "Accuracy of Compact-Stencil Interpolation Algorithms for Unstructured Mesh Finite Volume Solver," Heliyon, vol. 7, pp. e06875, 2021.

[3] A. Tasri, "Accuracy of Cell Centres to Vertices Interpolation for Unstructured Mesh Finite Volume Solver," Journal of the Institution of Engineers (India): Series C, vol. 102, pp. 577-584, 2021.

[4] T. J. Barth and D. C. Jespersen, "*The Design and Application of Upwind Schemes on Unstructured Meshes*," in AIAA 27th Aerospace Sciences Meeting, Reno,1989.

[5] W. K. Anderson and D. L. Bonhaus, "An Implicit Upwind Algorithm for Computing Turbulent Flows on Unstructured Grids," *Computers and Fluids*, vol. 23, pp. 1-21, 1994.

[6] J. A. White, H. Nishikawa, R. A. Baurle, "Weighted Least-Squares Cell-Average Gradient Construction Methods for the VULCAN-CFD Second-Order Accurate Unstructured Grid Cell-Centred Finite-Volume Solver," in AIAA *Scitech Forum*, (2019).

[7] H. Nishikawa, "Efficient Gradient Stencils for Robust Implicit Finite-Volume Solver Convergence on Distorted Grids," *Journal of Computational Physics*, vol. 386, pp. 486-501, 2019.

[8] S. S. Athkuri, V. Eswaran, "A New Auxiliary Volume-Based Gradient Algorithm for Triangular and Tetrahedral Meshes," *Journal of Computational Physics*, vol. 422, pp. 109780, 2020.

[9] S. S. Athkuri, M. R. Nived, V. Eswaran, "The Mid Point Green-Gauss Gradient Method and Its Efficient Implementation in A 3D Unstructured Finite Volume Solver," *International Journal for Numerical Methods in Fluids*, 2021.

[10] M. Aftosmis, D. Gaitonde and T. Tavares, "Behavior of Linear Reconstruction Techniques on Unstructured Meshes," *AIAA Journal*, vol. 11, pp. 2038-2049, 1995.

[11] D. Mavriplis, "*Revisiting the Least-Squares Procedure for Gradient Reconstruction on Unstructured Meshes*," in The 16th AIAA Computational Fluid Dynamics Conference, Florida, (2003).

[12] C. D. Correa, R. Hero and K. L. Ma, "A Comparison of Gradient Estimation Methods for Volume Rendering on Unstructured Meshes," IEEE Transactions on Visualisation and Computer Graphics, vol. 18, pp. 305-319, 2001.

[13] A. Syrakos, S. Varchanis, Y. Dimakopoulos, A. Goulas, J. Tsamopoulos, "A Critical Analysis of Some Popular Methods for the Discretisation of the Gradient Operator in Finite volume Methods, Physics of Fluids, vol. 29, pp. 12703, 2017.

[14] B. Diskin, J.L Thomas, "Comparison of Node-Centred and Cell-Centred Unstructured Finite-Volume Discretisations: Inviscid Fluxes," *AIAA Journal*, vol. 49, pp. 836-854, 2011.

[15] N. T. Frink, "Upwind Scheme for Solving the Euler Equations on Unstructured Tetrahedral Meshes," *AIAA Journal*, vol. 30, pp. 70-77, 1992.

[16] S. R. Mathur and J. T. Murthy, "A Pressure-Based Method for Unstructured Meshes," *Numer. Heat Transfer*, Part B, vol. 31, pp. 195-215, 9197.

[17] G. H. Golub and C. V. van Loan, "*Matrix Computations*," 3rd edition, London, The Johns Hopkins University Press, 1996.

[18] A. Tasri, "*Accuracy of Nominally 2nd Order, Unstructured Grid, CFD Codes*," PhD Thesis, University of Newcastle Upon Tyne, Newcastle, UK, 2005.

[19] F.M. White, "Fluid Mechanics," 8th Edition, New York, McGraw-Hill, 2015.

[20] N. Wang, M. Li, R. Ma, L. Zhang, "Accuracy Analysis of Gradient Reconstruction on Isotropic Unstructured Meshes and its Effects on Inviscid Flow Simulation," *Adv. Aerodyn.*, vol. 1, no. 1-31, 2019.

[21] B. Diskin, J. L. Thomasy, E. J. Nielsenz, H. Nishikawa, J. A. White, "Comparison of Node-Centered and Cell-Centered Unstructured Finite-Volume Discretisations, Part I: Viscous Fluxes," *AIAA Paper*, pp. 579, 2009.